



Performance Assessment of Hybrid Data Fusion and Tracking Algorithms

Stephan Sand, Christian Mensing, Mohamed Laaraiedh, Bernard Uguen, Benoît Denis, Sylvie Mayrargue, Mariano García, Javier Casajús-Quiros, Dirk Slock, Troels Pedersen, et al.

► To cite this version:

Stephan Sand, Christian Mensing, Mohamed Laaraiedh, Bernard Uguen, Benoît Denis, et al.. Performance Assessment of Hybrid Data Fusion and Tracking Algorithms. ICT mobile summit 2009, Jun 2009, Santander, Spain. hal-00486208

HAL Id: hal-00486208

<https://hal.science/hal-00486208>

Submitted on 2 Apr 2012

HAL is a multi-disciplinary open access archive for the deposit and dissemination of scientific research documents, whether they are published or not. The documents may come from teaching and research institutions in France or abroad, or from public or private research centers.

L'archive ouverte pluridisciplinaire **HAL**, est destinée au dépôt et à la diffusion de documents scientifiques de niveau recherche, publiés ou non, émanant des établissements d'enseignement et de recherche français ou étrangers, des laboratoires publics ou privés.

Performance Assessment of Hybrid Data Fusion and Tracking Algorithms

Stephan Sand¹, Christian Mensing¹, Mohamed Laaraiedh², Bernard Uguen², Benoît Denis³,
Sylvie Mayrargue³, Mariano García⁴, Javier Casajús⁴, Dirk Slock⁵, Troels Pedersen⁶,
Xuefeng Yin⁶, Gerhard Steinboeck⁶, Bernard H. Fleury⁶

¹ German Aerospace Center (DLR), Oberpfaffenhofen, 82234 Wessling, Germany

Email: {stephan.sand,christian.mensing}@dlr.de

² Université de Rennes 1, 35065 Rennes, France

³ CEA – Leti Minatec, 38054 Grenoble Cedex 9, France

⁴ Universidad Politecnica de Madrid, 28040 Madrid, Spain

⁵ Eurecom Institute, Sophia Antipolis 2229, 06560 Valbonne, France

⁶ Aalborg University, DK-9220 Aalborg, Denmark

Abstract: This paper presents an overview on the performance of hybrid data fusion and tracking algorithms evaluated in the WHERE consortium. The focus is on three scenarios. For the small scale indoor scenario with ultra wideband (UWB) complementing cellular communication systems, the accuracy can vary in time as a connectivity-dependent random process distributed over 3 orders of magnitude, from 100m in the worst situation down to 0.1m in the most favourable one. In the mid scale scenario, time difference of arrival (TDOA) measurements from a cellular network can give wide-area coverage with limited accuracy, whereas the received signal strength measurements of Wi-Fi hotspots give more accurate results if coverage is available. Finally, for large scale outdoor scenarios, cellular TDOA measurements can support global navigation satellite systems (GNSSs) especially in critical scenarios, where only a few satellites are visible. This is even the case when the overall accuracy of stand-alone cellular positioning is lower than that for GNSS positioning under optimum conditions.

Keywords: Positioning, hybrid data fusion, tracking, UWB, Wi-Fi, cellular communication systems, 3GPP-LTE, GNSS, TDOA, TOA, RSS, NLOS

1. Introduction

The main objective of the WHERE consortium [1] is to study radio positioning techniques using existing and future heterogeneous communication systems and to optimize the various layers of these systems, e.g., modulation, channel estimation and equalization, radio resource management, by exploiting the availability of reliable estimators for the position of mobile stations (MSs).

In order to provide reliable and accurate position information, the WHERE consortium researches hybrid data fusion (HDF) and tracking algorithms for positioning. For reliable positioning, it is necessary to exploit as much positioning information as possible. Typical measurements to compute the position of MSs include time of arrival (TOA), time-difference of arrival (TDOA), angle of arrival (AOA), received signal strength (RSS), Doppler frequency, or fingerprinting. Furthermore, different heterogeneous systems provide these position based measurements, e.g., cellular mobile radio communication systems, short range communication systems, or global navigation satellite systems (GNSSs). Potentially, each additional available measurement can improve the accuracy, availability, and reliability of the overall position solution.

In this paper, the WHERE consortium studies HDF and tracking algorithms to combine various measurements resulting in a single position solution. Additionally, we investigate tracking algorithms to improve the position accuracy and reliability of the MS, e.g., in point-to-point navigation.

2. Environments, Scenarios, and Sensor Models

For some environments, highly accurate positioning solutions are available already today. For instance, the positioning accuracy achieved by using the GNSS systems is in the range of a few meters in rural areas where several satellites can be seen line-of-sight (LOS) [2]. So, the focus in WHERE is on more challenging environments and scenarios [3].

The first scenario T1 addresses small-scale situations mainly in indoor environments where short-range ultra-wideband (UWB) links locally complement cellular systems such as the 3rd Generation Partnership Project Long Term Evolution (3GPP-LTE). Here, we consider the HDF of UWB TOA and 3GPP-LTE RSS measurements. We also evaluate the influence of LOS and non-line-of-sight (NLOS) propagation.

The second scenario T2 is a medium-scale indoor scenario, typically in an office-building. Here, RSS measurements of a Wi-Fi system complement TDOA measurements of a cellular 3GPP-LTE system. The indoor scenarios T1 and T2 have both in common that there is no GNSS available.

The third scenario T3 is a large-scale environment that considers GNSS, i.e., TOA measurements, and cellular 3GPP-LTE-based positioning, i.e., TDOA measurements, in urban canyon situations. Due to the availability of GNSS, the scenario T3 serves as a reference to compare the novel positioning methods developed in WHERE to already available approaches (cf. [4]). In all three scenarios, we assume pedestrian users.

In this paper, we consider RSS and timing based TOA and TDOA measurements: For the RSS sensor models (cf. [5], [6]), the RSS is usually modelled as a known constant transmit power multiplied by a random path loss, which accounts for the loss of signal strength due to the propagation from the transmitter to the receiver. Much effort has been devoted to the development of various path-loss models for communication purposes, especially with respect to the mobile radio channel. The path loss is commonly modelled as a stochastic variable with moments dependent on the distance. The randomness accounts for two effects: 1) the random propagation medium, and 2) the fading phenomena due to multipath propagation. However, when only few measurements are available, the RSS is sensitive towards especially small-scale fading.

For TOA models (cf. [7], [8], [9]) in free space, the TOA τ is related to the propagation distance via the speed of light c as $d = \tau \cdot c$. Estimation errors occur due to, e.g., clock drift, noise, interference, and propagation in heterogeneous environments, where multipath propagation and propagation via penetration occur.

3. HDF and Tracking Algorithms: Simulation Results

3.1 Scenario T1

The indoor location problem is far more unpredictable than that of outdoor GNSS where one can rely on a quasi deterministic underlying infrastructure. This remark is all the more valuable if considering positioning in mesh networks (e.g., impulse-radio UWB, as described in [5]) and when incorporating mobile-to-mobile range measurements. In the latter case, the positioning accuracy achievable at one mobile, even under HDF with cellular means, is indeed highly dependent on local connectivity with respect to other mobiles and/or anchor nodes (ANs), as well as on local mobility conditions.

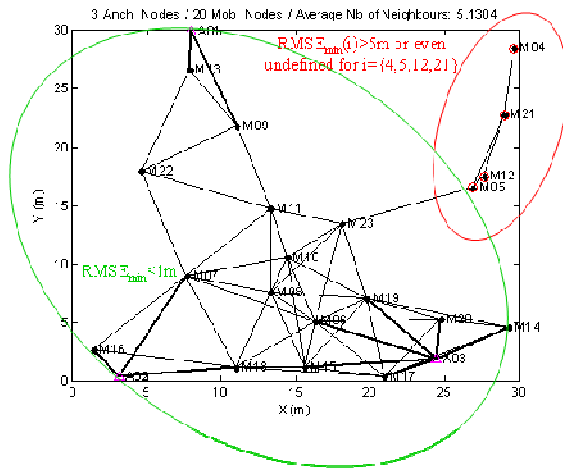


Figure 3-1: Illustration of poor (red-circled nodes) and favourable (green-circled nodes) local connectivity/rigidity on ideal position accuracy

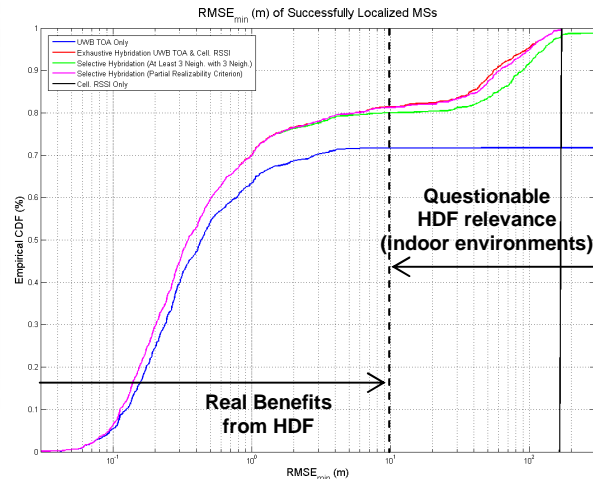


Figure 3-2: Empirical CDF of minimum 2D positioning RMSE for different UWB/Cellular HDF strategies

For example in Figure 3-1, we consider positioning 20 mobile nodes with respect to 3 ANs, in a $30\text{m} \times 30\text{m}$ 2D area at the center of a cellular sector with a maximum transmission range of 10m and a standard deviation of the TOA measurements taken as a random variable uniformly distributed over $[0, 0.3\text{m}]$ (e.g. [8]). The shadowing standard deviation of cellular measurements is constant and fixed at 8dB for all the nodes involved in the fusion procedure and incorporating the 3 strongest scanned RSSs with respect to available BS sectors. The shown curves are based on Monte Carlo realizations of the analytical conditional Cramer-Rao lower bound (CRLB) [5], [10].

From the cumulative distribution function (CDF) of 2D positioning errors shown in Figure 3-2, a clear gain for HDF in terms of both the positioning accuracy and location success rate, i.e., the average ratio of localizable nodes per network realization, is visible compared to no fusion as represented by the blue and black curves for UWB only and cellular 3GPP-LTE only. This is the case even with selective HDF strategies, which do not concern all the nodes but just the nodes preliminary identified as “unrealizable”. Selective HDF means that the nodes requiring HDF are selected according either to the “sub-graph partial realizability” criterion (magenta curve) or “at least 3 neighbours” criterion (green curve) [5]. Exhaustive HDF means the fusion with 3 cellular RSSs is systematically applied to all the nodes, without any prior selection (red curve). This selective HDF suffers from very slight degradations in comparison with the exhaustive fusion. The performance degradation starts becoming more noticeable in the “large-errors” regime, i.e., beyond a minimum root mean square error of 10m.

In this example, the gain is significant whatever the targeted position accuracy and whatever the selective fusion criterion. The benefits from HDF are pretty clear in the “small errors” regime, for instance with 70% of the nodes suffering from errors better than 1m, versus 64% when using only UWB means. The gain is also still evident in the “large errors” regime. For instance, 20% of the nodes suffer from positioning errors beyond 10m, but are still better than that of a pure LTE-enabled system. When relying only on UWB means, this percentage reaches 30%, with errors that can be even worse than that of a pure LTE-enabled positioning system. However, even if the positional accuracy available with HDF is always better than that of independent UWB or LTE systems, it might be more questionable for the initially claimed indoor environment, i.e., a $30\text{m} \times 30\text{m}$ area in the shown example. Indeed, at first sight, achieving a precision worse than the size of the explored geographic area where the mobile nodes are supposed to be located could look irrelevant. For this remaining portion of nodes that still enjoy errors worse than 10m even after HDF, it would

be worth reconsidering alternate or complementary positioning strategies or enhancing the fusion process itself. Hence, in a more general and typical indoor situation, one can predict that the accuracy will vary in time, as a random process barely distributed over 3 orders of magnitude, from 100m in the worst situation down to 0.1m in the most favourable one, which is mainly depending on local short-range connectivity.

Compared to state-of-the art HDF, the rigidity-aided HDF rules for positioning in heterogeneous communication networks provide simple but robust and MS based criteria to selectively activate HDF for nodes that have too few connections within one network. Hence, we achieve better positioning accuracy and better localizability overall independent of the node density.

In the remainder of this section, we investigate the influence of NLOS propagation and mitigation on HDF. The main effect of NLOS is to introduce biases in measurements, and a number of techniques have been proposed to mitigate this effect. In this paper, our approach incorporates the NLOS biases as additional “nuisance” parameters to be estimated using the observations. For instance, if we adopt a non-linear least-squares (LS) approach using TOA measurements, the problem of jointly finding positions and biases can be formulated as a constrained optimization problem as NLOS biases are always positive. Different non-linear programming tools can be used for its solution [11]; however, the probable existence of local minima on the error surface implies that, in some cases, an adequate solution cannot be reached, unless sufficient accurate a-priori knowledge of the node position is available.

When the node to be located is moving, we need to track the variability of its space coordinates with time. The position is, thus, described as a stochastic process to be estimated from the observations using a Bayesian decision-theoretic framework, and the usual minimum mean-square error (MMSE) or maximum a posteriori (MAP) optimization criteria can be used [12]. In most realistic mobility situations, a state-space model for the evolution of the kinematic parameters (position and, possibly, velocity) of the node is assumed, and the measurement equation is formulated according to the available information, e.g., RSS, TOA, or TDOA. If the model for the motion parameters is Markovian, a recursive estimation of the state variables can be performed; nevertheless, the non-linear nature of the relationship between position and measurements, and the fact that the errors are frequently non-Gaussian, usually preclude the use of simple, linear solutions to the filtering problem such as the Kalman filter, and so one must resort to higher complexity approaches, like the extended Kalman filter (EKF) [12] or the Rao-Blackwellized particle filter (RBPF) [13].

We have adopted a scenario consisting of a square room of $40\text{m} \times 40\text{m}$, with $N=6$ ANs located at the points of coordinates (0, 0), (40, 0), (0, 40), (40, 40), (0, 20), and (40, 20), respectively, and an MS moving according to a “random waypoint” mobility model [14] within the room. We will further assume that the ANs perform TOA measurements, but some of them are under NLOS conditions. The model for the measurement noise is taken from [7], which was obtained via ray-tracing tools assuming a bandwidth of 100 MHz. For this model, the measurement noise is Gaussian distributed with zero mean for LOS propagation and exponentially distributed with non-zero mean for NLOS propagation.

Figure 3-3 represents the simulation results obtained after 100000 time instants with sample interval $T=0.1$ (thus 10000 s simulated time). For comparison purposes, we have also plotted in Figure 3-3 the CDF of the location error when no NLOS bias mitigation is used, i.e., when the state vector only comprises the mobile position and velocity. We can see how considerably higher estimation errors are expected in this case.

Figure 3-4 represents the simulation results obtained after 100000 time instants with sample interval $T=0.1$ (thus 10000 s simulated time) and 6 ANs. We can see that the RBPF performs better than the EKF, but the differences are not very high because of the assumption of Gaussian process and measurement noises in the prediction and update

stages of the RBPF. Nevertheless, the key advantage of the RBPF over other estimators is that, as soon as a more refined knowledge of the likelihood functions is available, it can be readily incorporated into the update step to improve the whole estimation process.

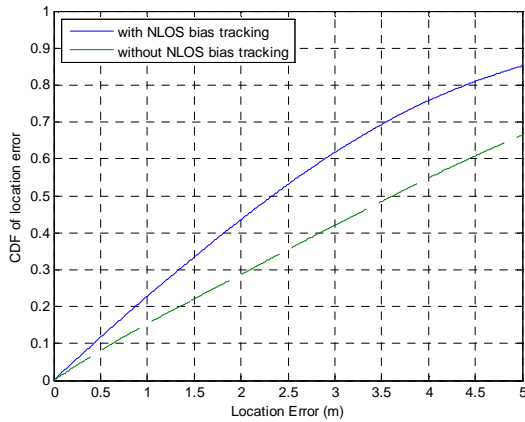


Figure 3-3: Distribution of the location error for EKF tracking

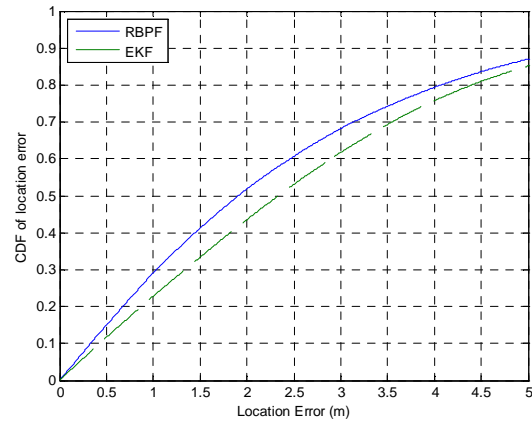


Figure 3-4: Distribution of the location error for EKF and RBPF tracking

Here, the innovation for NLOS mitigation is a reduced-complexity RBPF with NLOS bias tracking, in which we apply restrictions on the components of the particles. This substantially improves performance of RBPF over EKF.

3.2 Scenario T2

The Wi-Fi hotspots are randomly generated, where the noise for the RSS measurements is modelled as additive white Gaussian noise [5]. Figure 3-5 shows one generated environment with 200 hotspots/km² with a random coverage radius between 20m and 50m. Also depicted is a randomly generated MS track. Figure 3-6 shows the corresponding visibility of the hotspots depending on the MS position and the coverage of the hotspots. For this realization the number of visible hotspots varies between zero and four. For the cellular network coverage, we assume that the MS always receives signals from three BSs.

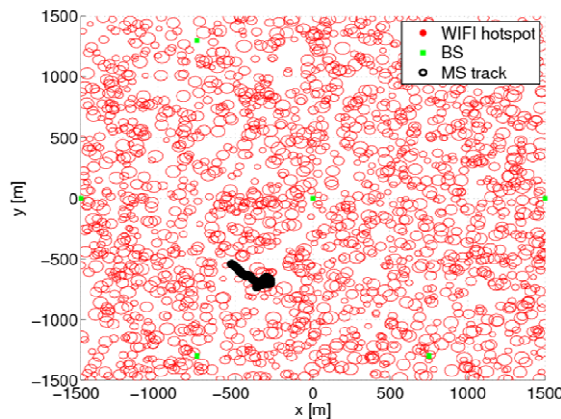


Figure 3-5: Scenario for positioning with Wi-Fi and cellular network

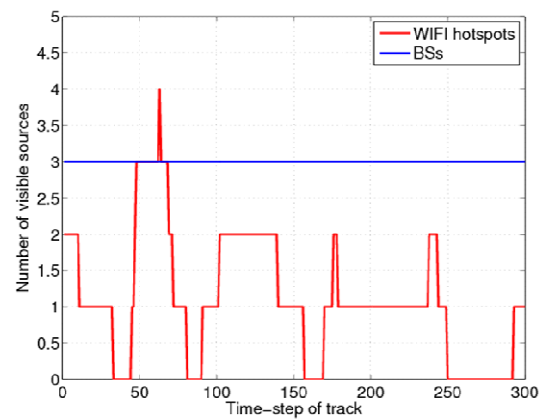


Figure 3-6: Number of visible sources (Wi-Fi hotspots and BSs) vs. time

The navigation equation is solved for a static MS using Wi-Fi hotspots, cellular BSs, or a combination of both with the Gauss-Newton algorithm [15]. Figure 3-7 and Figure 3-8 show the results for a density of 200 hotspots/km² and 100 hotspots/km². Considering Wi-Fi only positioning, it is usually required that the MS is in the coverage area of at least three hotspots. However, in case that less hotspots are visible to the MS the following procedure is applied: If no Wi-Fi hotspot is visible, no position solution can be provided. If one Wi-Fi

hotspot is visible, the estimate of the MS position is the position of the hotspot. If two Wi-Fi hotspots are visible, the two intersections of the two circles are determined. The estimate of the MS position is one of them (randomly chosen).

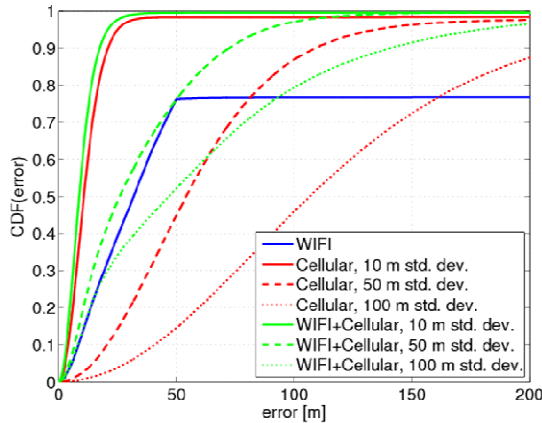


Figure 3-7: CDF for hybrid positioning using Wi-Fi and cellular network, Wi-Fi density of 200 hotspots/km²

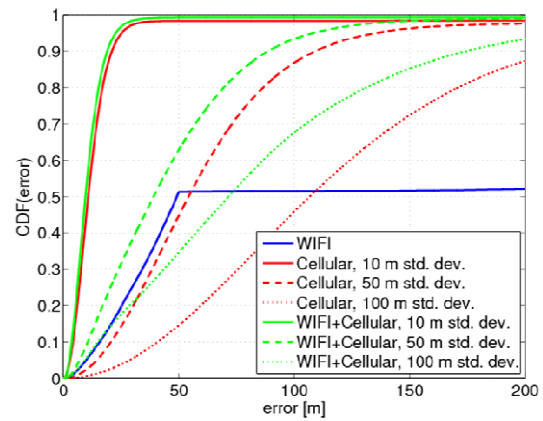


Figure 3-8: CDF for hybrid positioning using Wi-Fi and cellular network, Wi-Fi density of 100 hotspots/km²

This limits the position error to the Wi-Fi hotspot coverage area when at least one hotspot is visible. We observe that in around 24% of the situations no position can be provided for 200 hotspots/km². For 100 hotspots/km² this increases to 48%. However, when the MS is in the coverage area the position estimates are better than 50m, which reflects the maximum coverage range. The cellular network based TDOA measurements are also shown in these plots. The 90%-error is at around 23m for a standard deviation of 10m, at around 110m for a standard deviation of 50m, and at more than 200m for a standard deviation of 100m. However, the cellular network can provide a much better “global” coverage, and hence, availability than the Wi-Fi hotspots. Therefore, the hybrid solution combining Wi-Fi and cellular approaches can provide both reliability and availability.

System	CEP95	CEP90	CEP67
Wi-Fi	Not achievable	Not achievable	43m
TDOA (100m)	263m	215m	138m
TDOA (50m)	135m	109m	70m
TDOA (10m)	25m	20m	14m
Wi-Fi+TDOA (100m)	180m	140m	74m
Wi-Fi+TDOA (50m)	88m	72m	40m
Wi-Fi+TDOA (10m)	21m	17m	11m

Table 3.1: CEPs for different systems in T2 scenario using static solution; hotspot density of 200 hotspots/km²

For Scenario T2, the main results for a hotspot density of 200 hotspots/km² are summarized in Table 3.1. Whereas accuracy requirements on the position information exist for emergency calls, e.g., the CGALIES E-112 report [16] and the FCC E-911 requirements [17] in terms of $x\%$ circular error probability (CEP _{x}), there are no such requirements in the literature for exploiting position information in communications systems [18]. In Scenario T2, the achievable accuracy for different systems using the static solution is shown for CEP95, CEP90, and CEP67. We observe that the TDOA measurements from a cellular network can give wide-area coverage with limited accuracy, whereas the RSS measurements of Wi-Fi hotspots give more accurate results if coverage is available.

3.3 Scenario T3

In this scenario, we consider dynamic MSs, whose signals are fused and tracked with an EKF to obtain the position estimates [15]. For the dynamic MSs, we use a visibility model

of the satellites according to [5], [9]. In that model, the number of visible satellites changes every 10 time-steps according to (x = all visible, 4, 3, 2, 1, 0, 1, 2, 3, 4, all, 4, 3, etc.). The corresponding plot is shown in Figure 3-9. To evaluate the algorithms, different policies are possible to select the used satellites. We apply the highest elevation selection, i.e., the x satellites with the highest elevation are selected for positioning.

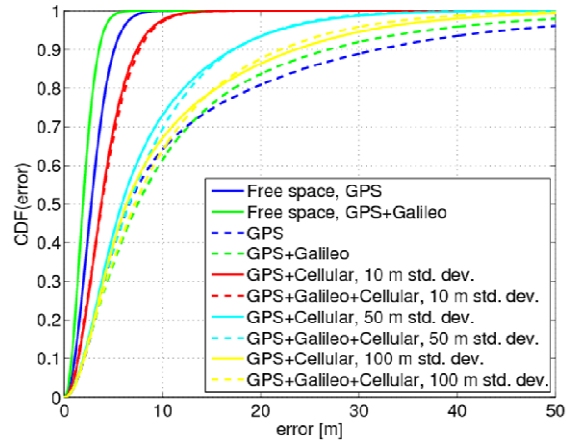
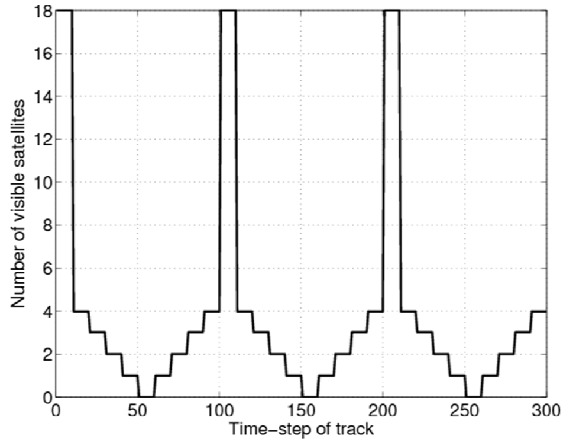


Figure 3-9: Number of visible GNSS satellites vs. time Figure 3-10: CDF for hybrid positioning using EKF

The HDF and EKF tracking curves where GNSS is combined with the cellular network are plotted in Figure 3-10 in terms of the CDF of the position error. We observe that depending on the quality of the TDOA estimates the average error can be reduced remarkably, especially in the critical situations. For instance, the 90%-error can be reduced from 32m (GPS) and 27m (GPS+Galileo) to around 22.5m (standard deviation 100m), 17m (standard deviation 50m), and 7.5m (standard deviation 10m).

System/environment	Free space			Urban canyon		
	CEP95	CEP90	CEP67	CEP95	CEP90	CEP67
GPS	5.9m	5.0m	3.5m	45m	32m	11m
GPS+Galileo	4.1m	3.0m	2.4m	37m	27m	11m
TDOA (100m)				65m	54m	36m
TDOA (50m)				38m	32m	22m
TDOA (10m)				11m	9m	6m
GPS+Galileo+TDOA (100m)				28m	22m	11m
GPS+Galileo+TDOA (50m)				22m	16m	9m
GPS+Galileo+TDOA (10m)				9m	8m	5m

Table 3.2: CEPs for different systems in T3 scenario using EKF tracking

For Scenario T3, the main results for EKF tracking are summarized in Table 3.2 for CEP95, CEP90, and CEP67. We see that cellular TDOA measurements can support GNSS especially in critical scenarios even if the overall accuracy of stand-alone cellular positioning is lower than for GNSS positioning under optimum conditions.

4. Conclusions

To conclude, this paper presents an overview on results for three scenarios. In the T1 Scenario, the position accuracy achieved with UWB TOA measurements complementing cellular 3GPP-LTE RSS measurements can vary from 100m in the worst case down to 0.1m in the best case. Despite the very inaccurate cellular RSS measurements, the HDF of UWB TOA and 3GPP-LTE RSS measurements can provide 10% more successful measurements with an accuracy of 10m or better. Compared to state-of-the art HDF, the rigidity-aided HDF rules for positioning in heterogeneous communication networks provide simple but robust and MS based criteria to selectively activate HDF for nodes that have too few connections within one network. Hence, we achieve better positioning accuracy and better

localizability overall independent of the node density. Further, NLOS estimation and mitigation in the T1 Scenario for the UWB TOA measurements yield a performance gain of 20% in terms of position estimates with a position error smaller than 5m. Here, the innovation for NLOS mitigation is a reduced-complexity RBPF with NLOS bias tracking, in which we apply restrictions on the components of the particles. This substantially improves performance of RBPF over EKF. In the T2 Scenario, cellular 3GPP-LTE-based TDOA measurements can provide wide-area coverage with limited accuracy, whereas the RSS measurements of Wi-Fi hotspots give more accurate results if coverage is available. Finally, for the T3 Scenario, cellular 3GPP-LTE-based TDOA measurements can support GNSS especially in urban canyons, where only a few satellites are visible. This is even the case when the overall accuracy of stand-alone cellular positioning is lower than that for GNSS positioning under optimum conditions.

For more details on current and future work of the WHERE project, we refer to [1] and [5].

5. Acknowledgment

This work has been performed in the framework of the ICT project ICT-217033 WHERE, which is partly funded by the European Union.

References

- [1] <http://www.ict-where.eu>
- [2] P. Misra and P. Enge, "Global Positioning System: Signals, Measurements, and Performance", Ganga-Jamuna Press, 2004.
- [3] WHERE Project, ICT-217033, Deliverable D1.1, "Definition of the WHERE framework and scenarios", March 2008.
- [4] GREAT Project, "Galileo Receivers for Mass-Market (GREAT)", <http://www.greatproject.org>, September 2008.
- [5] WHERE Project, ICT-217033, Deliverable D2.1, "Performance assessment of hybrid data fusion and tracking algorithms", December 2008.
- [6] A. Goldsmith, "Wireless Communications", Cambridge University Press, New York, NY, USA, 2005.
- [7] B. Alavi and K. Pahlavan, "Bandwidth Effect on Distance Error for Indoor Geolocation", Proc. IEEE PIMRC'03, Sept. 2003.
- [8] D. Lachartre, B. Denis, D. Morche, L. Ouvry, M. Pezzin, B. Piaget, J. Prouvé, P. Vincent, "A 1.1nJ/bit 802.15.4a-Compliant Fully Integrated UWB Transceiver in 0.13 μ m CMOS", IEEE ISSCC'09, San Francisco, Feb. 2009.
- [9] ESA, "Galileo System Simulation Facility (GSSF)", <http://www.gssf.info/>, January 2007.
- [10] S. M. Kay, "Fundamentals of Statistical Signal Processing, Volume 1: Estimation Theory", Prentice Hall Signal Processing Series, 1993.
- [11] K. Yu and Y. J. Guo, "Efficient Location Estimators in NLOS Environments", Proc. IEEE PIMRC'07, Sep. 2007.
- [12] F. Gustafsson and F. Gunnarsson, "Mobile Positioning Using Wireless Networks", IEEE Signal Processing Magazine, July 2005.
- [13] T. Schön, F. Gustafsson, and P.-J. Nordlund, "Marginalized Particle Filters for Mixed Linear/Nonlinear State-Space Models", IEEE Trans. on Signal Processing, pp. 2279-2289, July 2005.
- [14] T. Camp, J. Boleng and V. Davies, "A Survey of Mobility Models for Ad Hoc Network Research", Wireless Communication & Mobile Computing (WCMC), vol. 2, no. 5, pp. 483-502, 2002.
- [15] C. Mensing and S. Plass, "Positioning Algorithms for Cellular Networks Using TDOA", Proceedings of the IEEE ICASSP'06 Toulouse, France, May 2006.
- [16] Coordination Group on Access to Location Information for Emergency Services (CGALIES), "Final Report: Report on Implementation Issues Related to Access to Location Information by Emergency Services (E112) in the European Union", <http://www.telematica.de/cgalies/>, February 2002.
- [17] Federal Communications Commission, "FCC 99-245: Third Report and Order", <http://www.fcc.gov/911/enhanced/>, October 1999.
- [18] WHERE Project, ICT-217033, Deliverable D6.2, "Survey on Localisation in Communication Networks", October 2008.